



Lawrence Berkeley Laboratory

UNIVERSITY OF CALIFORNIA

Accelerator & Fusion Research Division

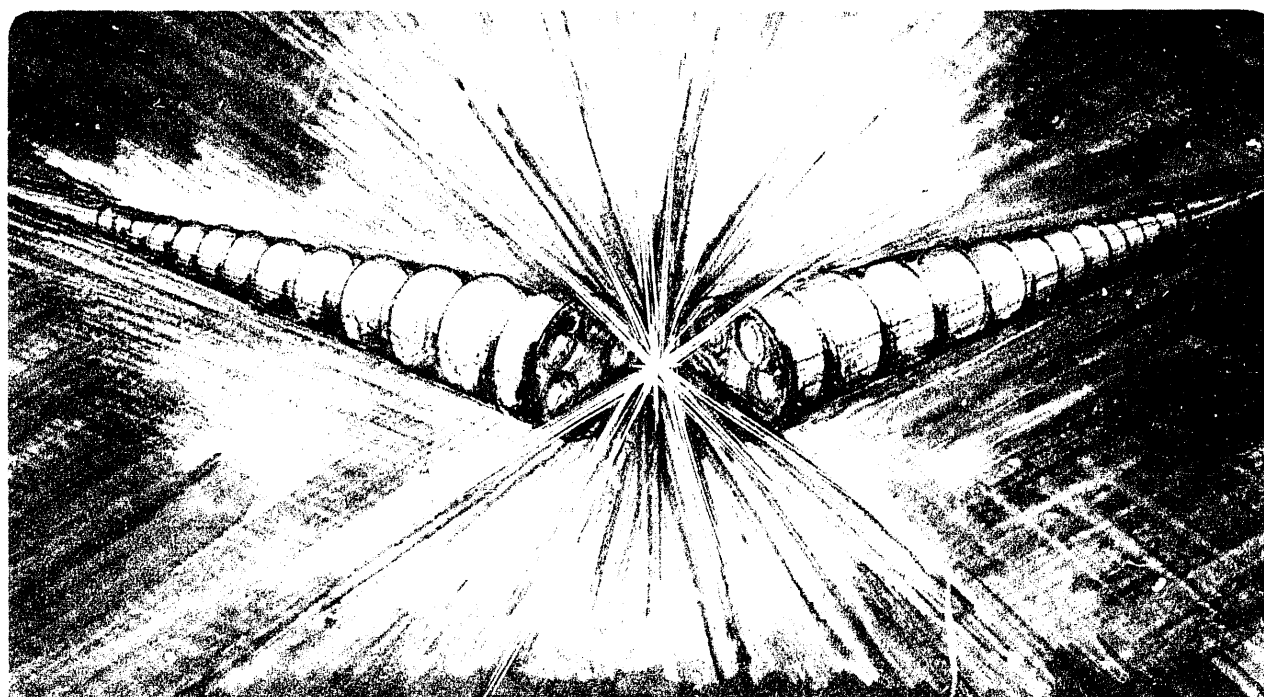
Received by OSTI

DEC 16 1991

Beam-Beam Dynamics During the Injection Process at the PEP-II B-Factorv

Y.H. Chin

October 1991



Prepared for the U.S. Department of Energy under Contract Number DE-AC03-76SF00098

DISTRIBUTION OF THIS DOCUMENT IS UNLIMITED

DISCLAIMER

This document was prepared as an account of work sponsored by the United States Government. Neither the United States Government nor any agency thereof, nor The Regents of the University of California, nor any of their employees, makes any warranty, express or implied, or assumes any legal liability or responsibility for the accuracy, completeness, or usefulness of any information, apparatus, product, or process disclosed, or represents that its use would not infringe privately owned rights. Reference herein to any specific commercial product, process, or service by its trade name, trademark, manufacturer, or otherwise, does not necessarily constitute or imply its endorsement, recommendation, or favoring by the United States Government or any agency thereof, or The Regents of the University of California. The views and opinions of authors expressed herein do not necessarily state or reflect those of the United States Government or any agency thereof or The Regents of the University of California and shall not be used for advertising or product endorsement purposes.

Lawrence Berkeley Laboratory is an equal opportunity employer.

Beam-Beam Dynamics During the Injection Process at the PEP-II B-Factory *

LBL--31434

DE92 004097

Yong Ho Chin

Exploratory Studies Group
Accelerator & Fusion Research Division
Lawrence Berkeley Laboratory, Berkeley, CA 94720

I. Introduction

This paper is concerned with beam-beam effects during the injection process at the proposed asymmetric SLAC/LBL/LLNL B-Factory based on PEP (PEP-II) [1]. For symmetric colliders, the primary source of the beam-beam effect is the head-on collision at the interaction point (IP), and this effect can be mitigated by separating the beams during the injection process. For an asymmetric collider, which intrinsically consists of two separate rings, the bunches not only collide at the IP but experience a long-range beam-beam force on the way into and out of the IP region (where both beams travel in a common vacuum pipe). These collisions are called "parasitic crossings (PC)." The parasitic crossings emerge as a potential source of far stronger beam-beam impact during the injection process for the following reason. In the proposed injection scheme of the APIARY-6.3d design [1], the bunches are injected horizontally into the two rings with large horizontal offset of $8\sigma_{0x}^{sptm}$ where σ_{0x}^{sptm} is the nominal horizontal storage ring beam size at the end of the septum magnet. Then, the injected beam starts to travel around the ring oscillating horizontally. For the sake of discussion, let us assume that the beam in the other ring has already been fully stored. When the injected beam arrives at the 1st PC, where the two nominal orbits are separated horizontally by about 7.6 times the nominal horizontal beam size of the low energy ring (LER), it may pass through the other beam far more closely than at the nominal separation distance, or it may even strike the other beam head-on. Due to the large vertical beta function (~ 20

* This work was supported by the Director, Office of Energy Research, Office of High Energy and Nuclear Physics, High Energy Physics Division, of the U.S. Department of Energy under Contract No. DE-AC03-76SF00098.

DISTRIBUTION OF THIS DOCUMENT IS UNLIMITED



MASTER

m), the vertical beam-beam tune shift at the 1st PC can become of the order of unity in the head-on collision case, which is larger than the normal beam-beam tune shift limit by one or two orders of magnitude. Although these “close encounters” take place only irregularly owing to the non-integer betatron tunes, and the coherent oscillation of the injected beam itself dies out gradually due to radiation damping, the occasional strong impact at an early stage of the injection process may lead to a significant blowup of the injected beam and to a subsequent particle loss. We carry out simulations to see if the proposed horizontal injection scheme gives acceptable performance. Throughout this paper we assume that the injection takes place into the low energy ring and that the beam in the high energy ring (HER) has already been fully stored. This configuration is expected to give the worst case with respect to the beam dynamics, since previous studies on the beam-beam interaction including the PC in APIARY-6.3d [1,2,3] show that it is the low energy beam that mostly blows up.

Hutton [4] has pointed out that when the injected beam collides with the counter-rotating beam at the PC, particles in the injected beam receive horizontal kicks whose sign depends on whether the particle is located in the inner side or the outer side with respect to the center of the other beam in horizontal phase space. This is illustrated in Fig. 1. The result is that the beam will have a tendency to shear into an elongated shape and eventually to spread out over a circular annulus. This will lead to a damping of the horizontal baricentroid motion even though the particle amplitudes themselves have not yet been significantly damped. It will be shown that the present simulation results support this idea.

Other injection schemes have been suggested to avoid the strong parasitic interaction during the injection process. One such scheme is to inject beams vertically instead of horizontally. Obviously, this scheme prevents the injected beam from approaching the other beam at the PC closer than the nominal separation distance between the two stored-beam orbits at the PC. Another scheme is horizontal injection with vertical separation at both the IP and the PC by creating a temporary bumped orbit during the injection. We examine these two injection schemes as well.

II. Horizontal Injection

The main storage ring and injection parameters of APIARY-6.3d and those values at the IP and the first PC are listed in Table 1. Of six PC's near the IP, we consider

only the 1st PC (the one closest to the IP) on either side, because it overwhelms the others in terms of the strength of the beam-beam kick on account of the small separation and the large vertical beta function. The injection parameters are specified in square brackets.

Table 1. The main storage ring and injection parameters of APIARY-6.3d.
The injection parameters are specified in square brackets.

	Low Energy Ring (LER, e^+)		High Energy Ring (HER, e^-)	
Energy, E (GeV)	3.1		9	
Circumference, C (m)	2200		2200	
Damping time, $\tau_x = \tau_y$ (turns)	5070		4970	
Bunch current, I_b (mA)	1.23 [0.246]		0.848	
Bunch Length, σ_s (cm)	1.0		1.0	
Nominal emittance				
ϵ_{0x} (nm-rad)	92 [8.24]		46	
ϵ_{0y} (nm-rad)	3.6 [8.24]		1.8	
Separation distance at the 1st PC, d_x (mm)			2.82	
	IP	1st PC	IP	1st PC
Beta function,				
β_x (m)	0.375	1.51	0.75	1.30
β_y (m)	0.015	25.23	0.03	13.01
Nominal rms beam size				
σ_{0x} (μm)	186 [56]	373 [112]	186	245
σ_{0y} (μm)	7.4 [11.2]	302 [457]	7.4	153
d_x/σ_{0x}	–	7.3 [25.2]	–	11.5
Physical aperture,				
A_x/σ_{0x}	10		10	
A_y/σ_{0y}	36		36	

A bunch with 20% of the nominal single-bunch current is injected to the LER with a horizontal displacement $8\sigma_{0x}^{sptm}$ from the stored beam orbit, where σ_{0x}^{sptm} is the nominal horizontal beam size of the LER at the end of the septum magnet. We assume that the phase advance between the injection point and the IP is 2π times an integer. The configuration is sketched in Fig. 2. We have selected the fractional tunes of the working point to be $\delta Q_x = 0.64$ and $\delta Q_y = 0.57$ for both beams.

Figure 3 shows the rms sizes of the injected beam in units of the nominal storage ring beam sizes versus the turn number after the injection. The largest turn number, 10000, corresponds to about 2.3 radiation damping times. The characters “x” and “y” denote the relative horizontal and vertical beam sizes, respectively, while the character “o” represents the rms bunch length in units of the nominal value. We can see that the vertical beam size reaches its peak value very quickly within approximately 300 turns, since the near-head-on collisions of the two beams soon after the injection scattered the injected beam vertically. The beam blowup then damps out gradually in the following few radiation damping times. The horizontal beam size also blows up, much more slowly however, to about 3 times the nominal storage ring value, roughly within one radiation damping time. Despite the large vertical beam blowup, no particle loss out of 200 “superparticles” was found during the simulation. The high energy beam sizes, which are not plotted here, show practically no change from their nominal values.

Let us investigate the behavior of the horizontal distribution of the injected beam in detail. As mentioned in the Introduction, it is expected that an injected beam forms a circular annulus in horizontal phase space due to a shearing force from the other beam, and consequently, the horizontal baricentroid motion of the injected beam damps out faster than the damping of the amplitudes of individual particles. Figure 4 shows the evolution of the baricentroid motion of the injected beam. The characters “x” and “y” denote the horizontal and the vertical baricentroid positions (in units of the nominal storage ring beam size) sampled at the IP every 172 turns, respectively. In Figs. 5(a)-(e), we plot the horizontal distribution of the injected beam in normalized phase space at the five sequential points in time, 0, 1000, 2000, 3000, and 4000 turns after the injection, respectively. Note that the initial horizontal size of the injected beam is about 30% of that of the nominal storage ring beam size. The phase space distribution at 1000 turns shown in Fig. 5(b) already forms a crescent shape due to the shearing force. The annulus is closed within 4000 turns (see Fig. 5(e)) or roughly within one

radiation damping time. Accordingly, the horizontal baricentroid position settles down at the origin as shown in Fig. 4. This process will be likely to be accelerated if the amplitude dependent tune shift due to lattice nonlinearities are taken into account. The above behavior of the injected beam is consistent with Hutton's explanation.

III. Vertical Injection

Although the simulation result of the horizontal injection shows no particle loss despite the large vertical beam blowup of the injected beam, we intend to explore alternative solutions that can maintain good performance in terms of the beam blowup and particle loss even in the presence of machine errors or injection errors. As mentioned in the Introduction, the strong parasitic beam-beam interaction results from the "close encounters" at the PC due to the horizontal coherent oscillation of the injected beam. It is therefore natural to think of vertical instead of horizontal injection. In this case, for geometrical reasons, the two beams cannot get closer at the PC than the nominal separation distance. The beam-beam kick is accordingly much weaker on average. However, the parasitic beam-beam interaction, being a collision of the two beams at large amplitude in phase space, still tends to shear the injected beam into an elongated shape, in vertical phase space in this case. The process is accelerated as the vertical coherent oscillation of the injected beam damps away and, as a result, the distance between the two beams gets shorter on average. This is schematically illustrated in Fig. 6. This is a peculiar point in contrast to the horizontal injection case where the parasitic beam-beam interaction becomes weaker as the horizontal coherent oscillation of the injected beam damps away. However, the parasitic beam-beam interaction in both cases approaches the same strength in the final steady-state.

Since the design of the vertical injection scheme is not complete, we assume at the present time that the vertical offset of the injected beam from the stored beam orbit at the injection point is 8 times the vertical rms beam size of the LER (at full x-y coupling) at that point. This offset corresponds to 28.8 times the nominal vertical beam size if an x-y coupling of 0.04 is assumed. The full-coupling beam size is used because that is what determines the physical aperture.

Figure 7 shows the time evolution of the injected beam sizes (normalized to the nominal storage ring beam sizes) up to 20000 turns. The evolution of the baricentroid motion of the injected beam is shown in Fig. 8. The notations follow those in Sec.

II. No particle loss was found during the simulation. In Figs. 9(a), (b) and (c), we plot the vertical phase space distribution of the injected beam after 4000, 8000, and 10000 turns, respectively. Figure 9(a) is a typical phase space distribution at an early stage of the simulation where the injected beam is slowly sheared into an elongated shape. The vertical beam size fluctuates around the value $\sim 3.5\sigma_{0y}$ in balance between two conflicting tendencies, namely, the shearing movement to increase the rms beam size, and the damping of the coherent oscillation of the injected beam to decrease it. Finally, the elongated shape is closed to a circular annulus after approximately 8000 turns as shown in Fig. 9(b). The vertical beam size then reaches its maximum value, $\sim 4.5\sigma_{0y}$. The vertical baricentroid motion dies out at the same time. At this point, the rotational shearing movement in vertical phase space does not contribute to the change in the vertical rms beam size, and the injected beam converges monotonically toward its equilibrium sizes due to radiation damping.

IV. Horizontal Injection with Vertical Separation

One potential advantage of horizontal injection over vertical injection is that it allows more space to place the injection equipment since the two rings are located one atop the other. To mitigate the effect of the near-head-on collision of the two beams at the PC, it is possible to separate the beams vertically at the PC, as well as at the IP, for instance, by creating a temporary vertically bumped orbit. The penalty in this case is that it may introduce new complications, such as avoiding excessive beam blowup during the restoration of the bumped orbit. Obviously, if the separation is large enough, the effect of the PC diminishes. Therefore, the question lies in how much separation we need for acceptable performance. We assume that the bumped orbit for the vertical separation is designed in such a way that the new orbit is shifted in the same direction at the IP and the PC in one ring, but the direction is opposite in the other ring. In this way we can naturally have a separation at the IP as well as at the PC. We also assume that the vertical separation at the IP is $\pm 2\sigma_{0x}^*$ where σ_{0x}^* is the nominal horizontal storage ring beam size at the IP. The adequacy of this separation distance is based on experimental results at PEP [5].

In Figs. 10(a)-(d), we plot the time evolution of the relative sizes of the injected beam when the separation d_y at the PC is, (a) $4\sigma_{0x,+}$, (b) $6\sigma_{0x,+}$, (c) $8\sigma_{0x,+}$, and (d) $9\sigma_{0x,+}$, respectively, where $\sigma_{0x,+}$ is the horizontal nominal rms beam size of the LER at

the PC and all the other parameters are kept fixed. The corresponding absolute values of d_y are (a) 1.488 mm, (b) 2.232 mm, (c) 2.976 mm, and (d) 3.348 mm, respectively. From Figs. 10(c) and (d), we notice that there is little or no vertical beam blowup for a separation $d_y \geq 8\sigma_{0x,+}$. Recall that the initial vertical and horizontal beam sizes of the injected beam are about 1.5 and 0.3 times the nominal LER beam sizes, respectively. The relatively small overshoot of the horizontal beam size is caused by the smearing effect in horizontal phase space due to the tune dependence on amplitude produced by the residual parasitic beam-beam force. Additional smearing associated with magnetic imperfections is also to be expected. The beam dynamic behavior is now very close to nominal.

V. Conclusions

We have investigated the beam-beam effects during the injection process including the effect of the parasitic crossings, for the APIARY-6.3d design of the PEP-II B-Factory. It is found that the strong parasitic beam-beam interaction in the proposed horizontal injection scheme can induce a significant beam blowup in the vertical size of the injected beam, although it does not appear to lead to particle loss. Although the resultant performance should still be acceptable, we have explored two other injection schemes in an attempt to seek a solution that entails less blowup of the injected beam size. The simulation results for both (1) a vertical injection scheme and (2) a horizontal injection scheme with vertical separation at the IP and PC show substantial improvements in terms of the blowup of the injected beam sizes. In the second case, it is found that the beam blowup due to the parasitic crossings can even be eliminated for a vertical separation $d_y \geq 8\sigma_{0x,+}$ at the PC, where $\sigma_{0x,+}$ is the nominal horizontal rms beam size of the LER at the PC. In this case, the beam dynamic behavior becomes almost nominal. It is interesting to point out that this criterion is similar to one previously obtained for the horizontal separation at the PC [2], namely $d_x \geq 7\sigma_{0x,+}$, that mitigates the effects of the parasitic crossings in the collision mode.

Acknowledgments

The author would like to thank M. Zisman and A. Hutton for suggesting this problem and helpful discussions. He also would like to thank M. Furman for helpful discussions and careful proofreading of the manuscript.

References

1. *An Asymmetric B Factory Based on PEP, Conceptual Design Report*, Lawrence Berkeley Laboratory Report LBL PUB-5303/SLAC-372/CALT-68-1715/UCRL-ID-106426/UC-IIRPA-91-01, February 1991.
2. Y. H. Chin, to be published in *Proc. of the IEEE Particle Accelerator Conference* (San Francisco, CA, May 6-9, 1991); Lawrence Berkeley Laboratory Report LBL-30701, May 1991.
3. M. A. Furman, Lawrence Berkeley Laboratory Report LBL-30981/ESG Note-144/ABC-44, September 1991.
4. A. Hutton, SLAC Memorandum, June 1991.
5. The SPEAR Group, in *Proc. of the IXth International Conference on High Energy Accelerators* (Stanford Linear Accelerator Center, Stanford, CA, May 2-7, 1974), p.66.

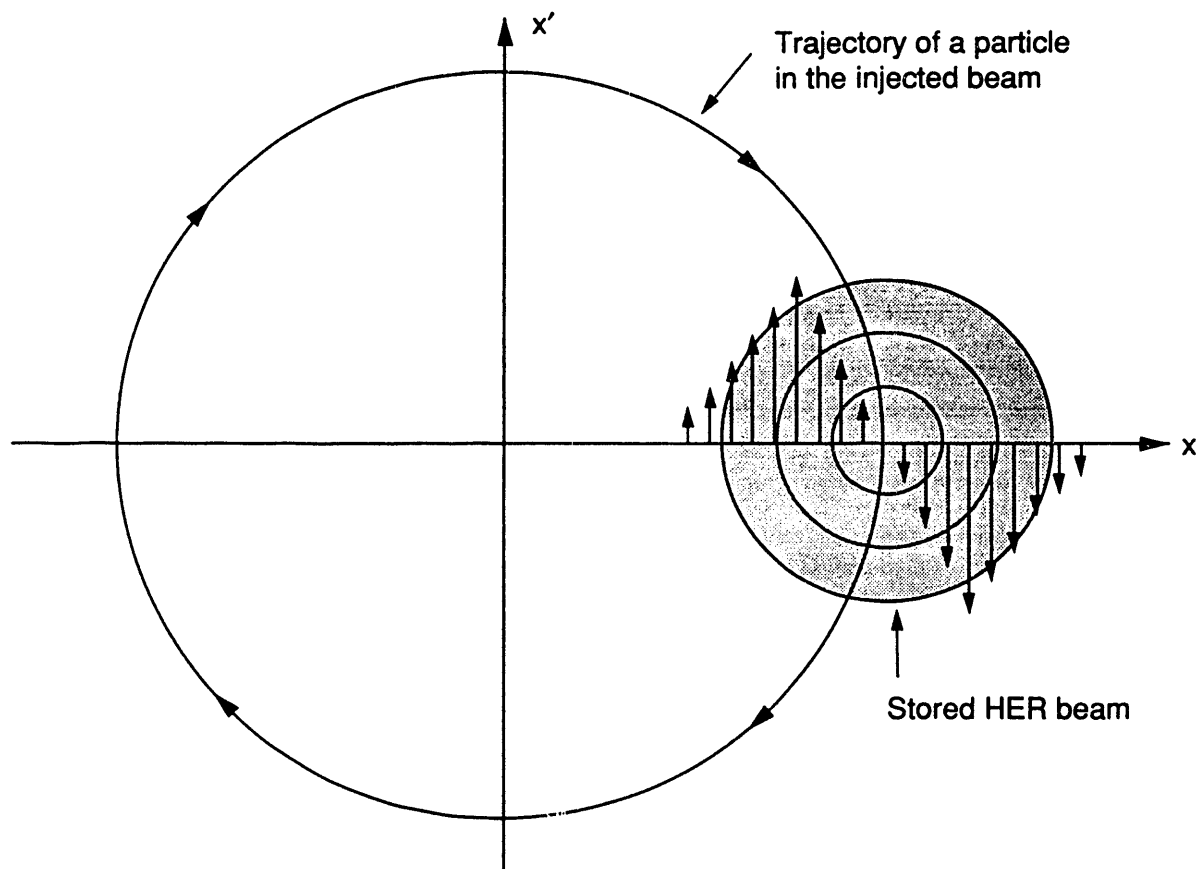


Figure 1. Schematic illustration of the parasitic beam-beam interaction in horizontal phase space. Particles in the injected beam receive a horizontal kick whose sign depends on whether the particle is located in the inner side or the outer side with respect to the center of the stored beam, represented by the shaded circle.

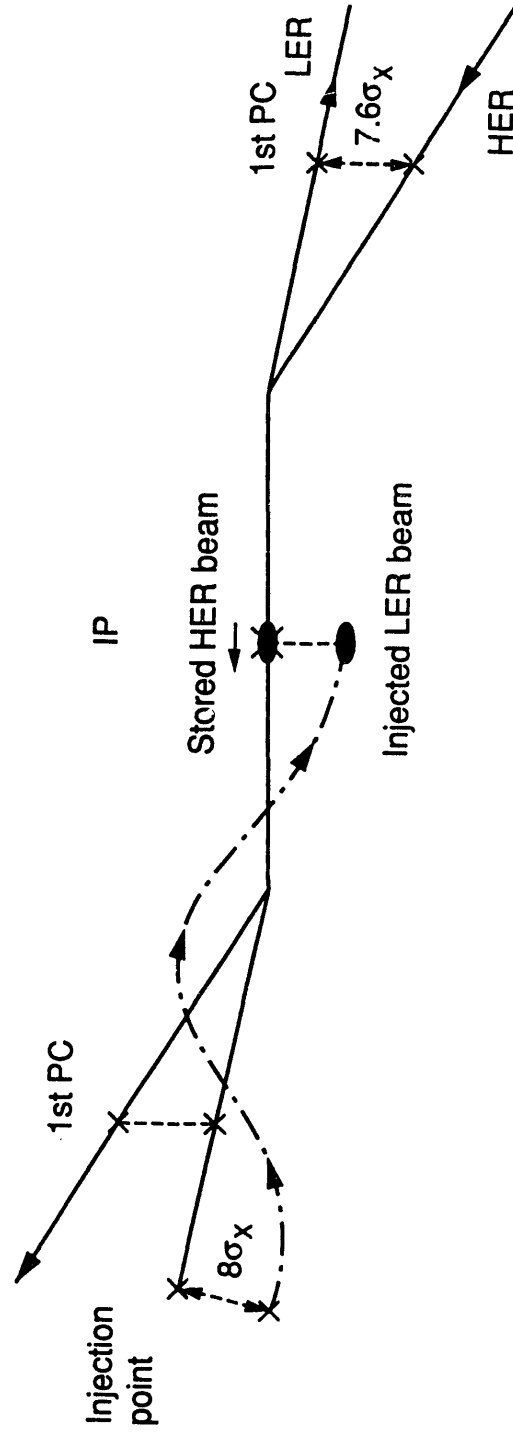


Figure 2. Sketch of the horizontal injection configuration.

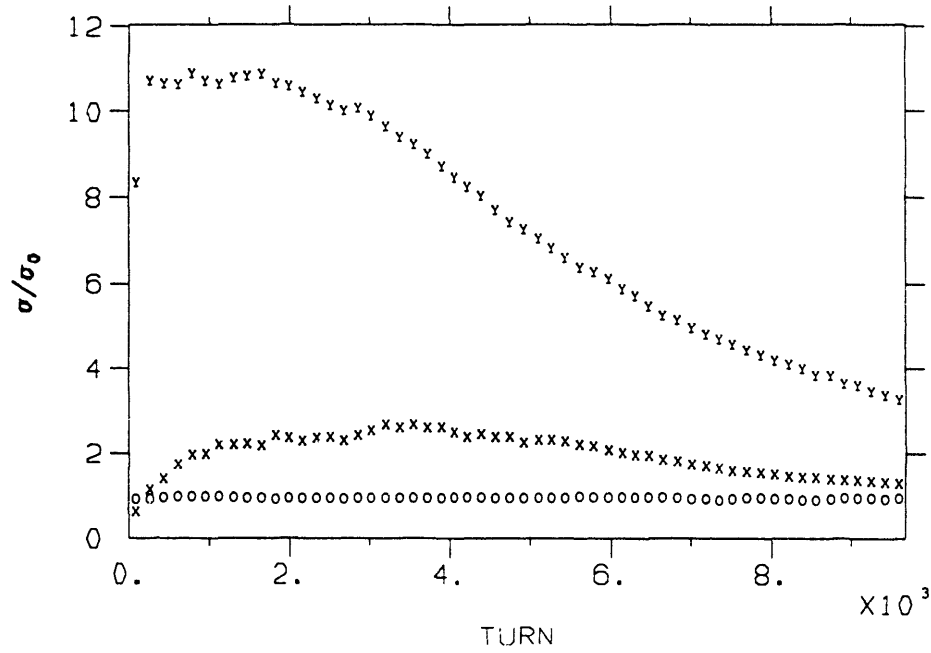


Figure 3. The time evolution of the injected beam sizes in units of the nominal storage ring beam sizes during the horizontal injection process (x=horizontal, y=vertical, and o=longitudinal).

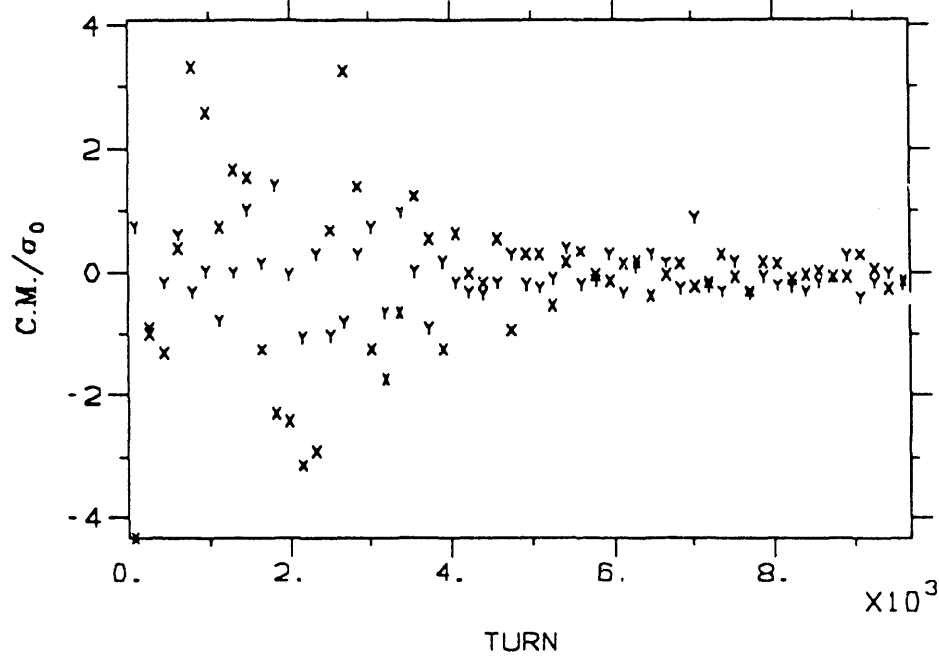


Figure 4. The time evolution of the baricentroid positions of the injected beam in units of the nominal storage ring beam sizes during the horizontal injection process (x=horizontal, and y=vertical).

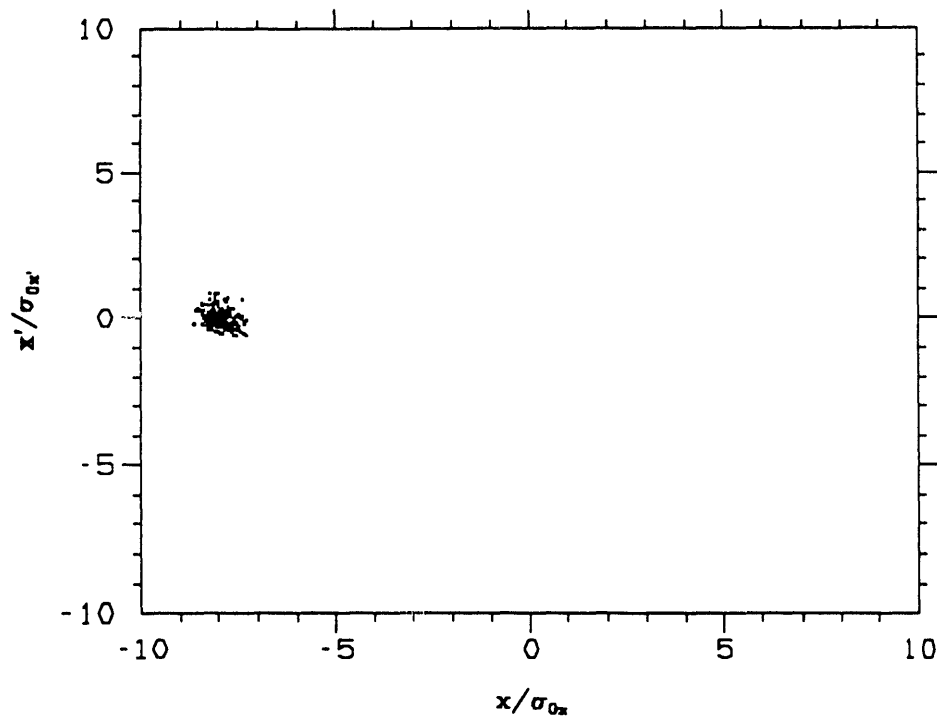


Figure 5(a). The horizontal distribution of the injected beam in normalized phase space soon after horizontal injection.

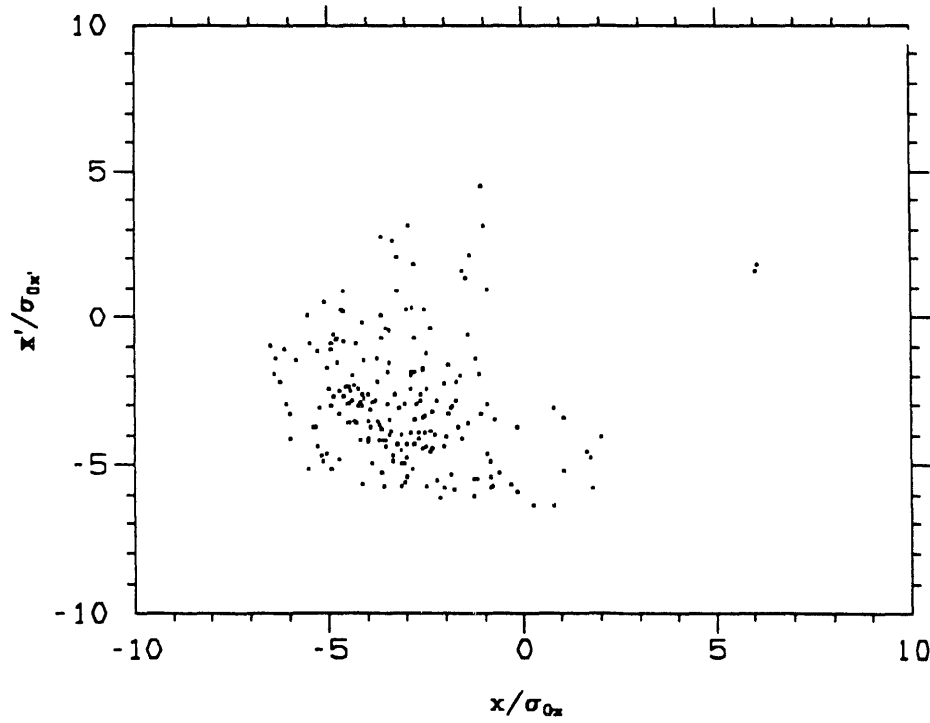


Figure 5(b). The horizontal distribution of the injected beam in normalized phase space after 1000 turns.

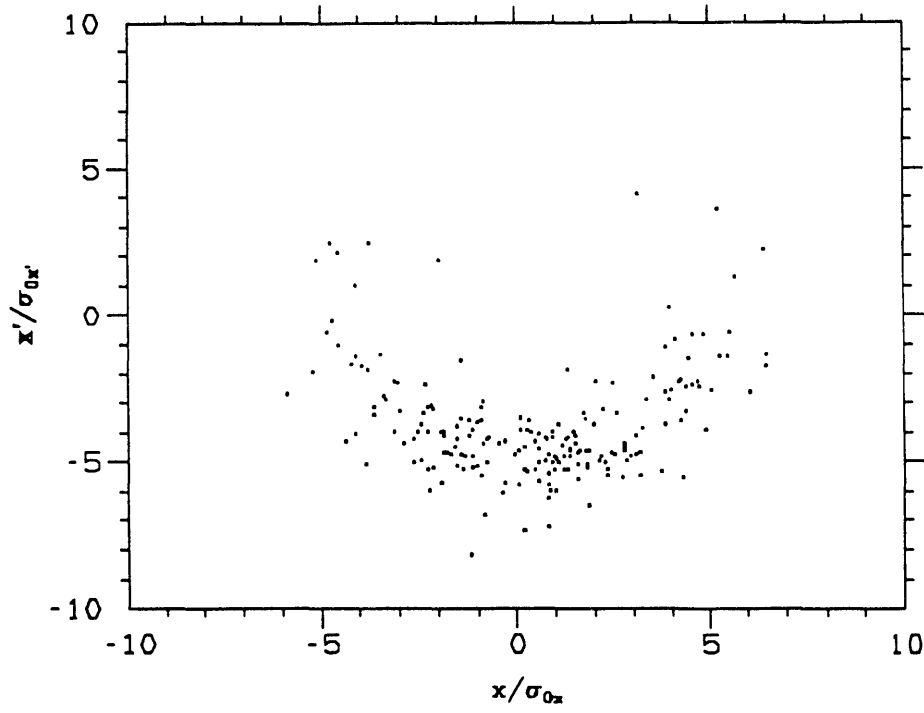


Figure 5(c). The horizontal distribution of the injected beam in normalized phase space after 2000 turns.

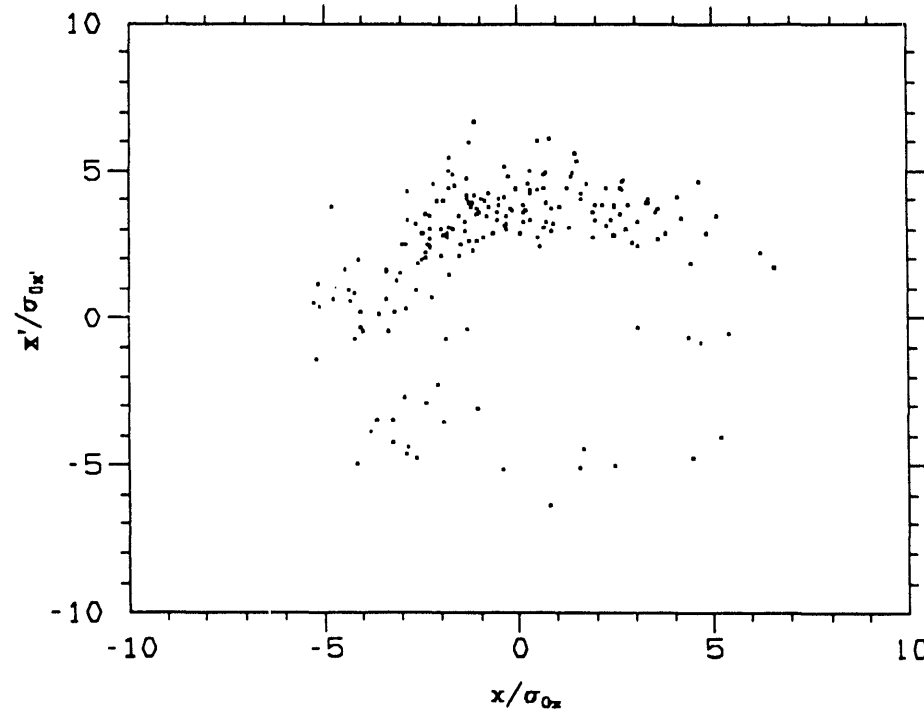


Figure 5(d). The horizontal distribution of the injected beam in normalized phase space after 3000 turns.

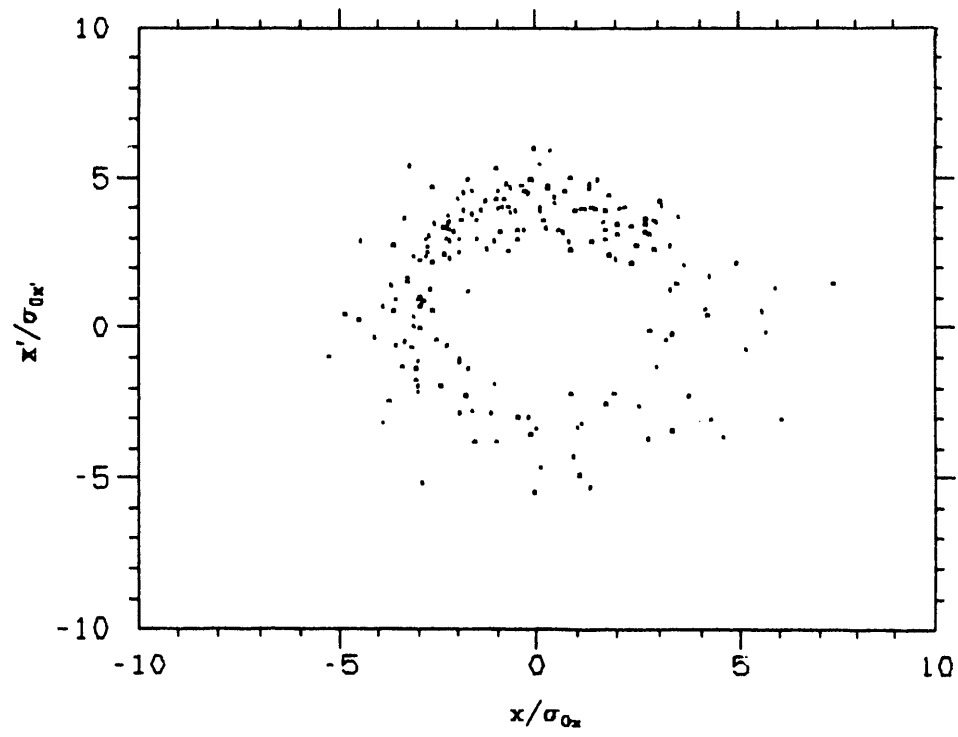


Figure 5(e). The horizontal distribution of the injected beam in normalized phase space after 4000 turns.

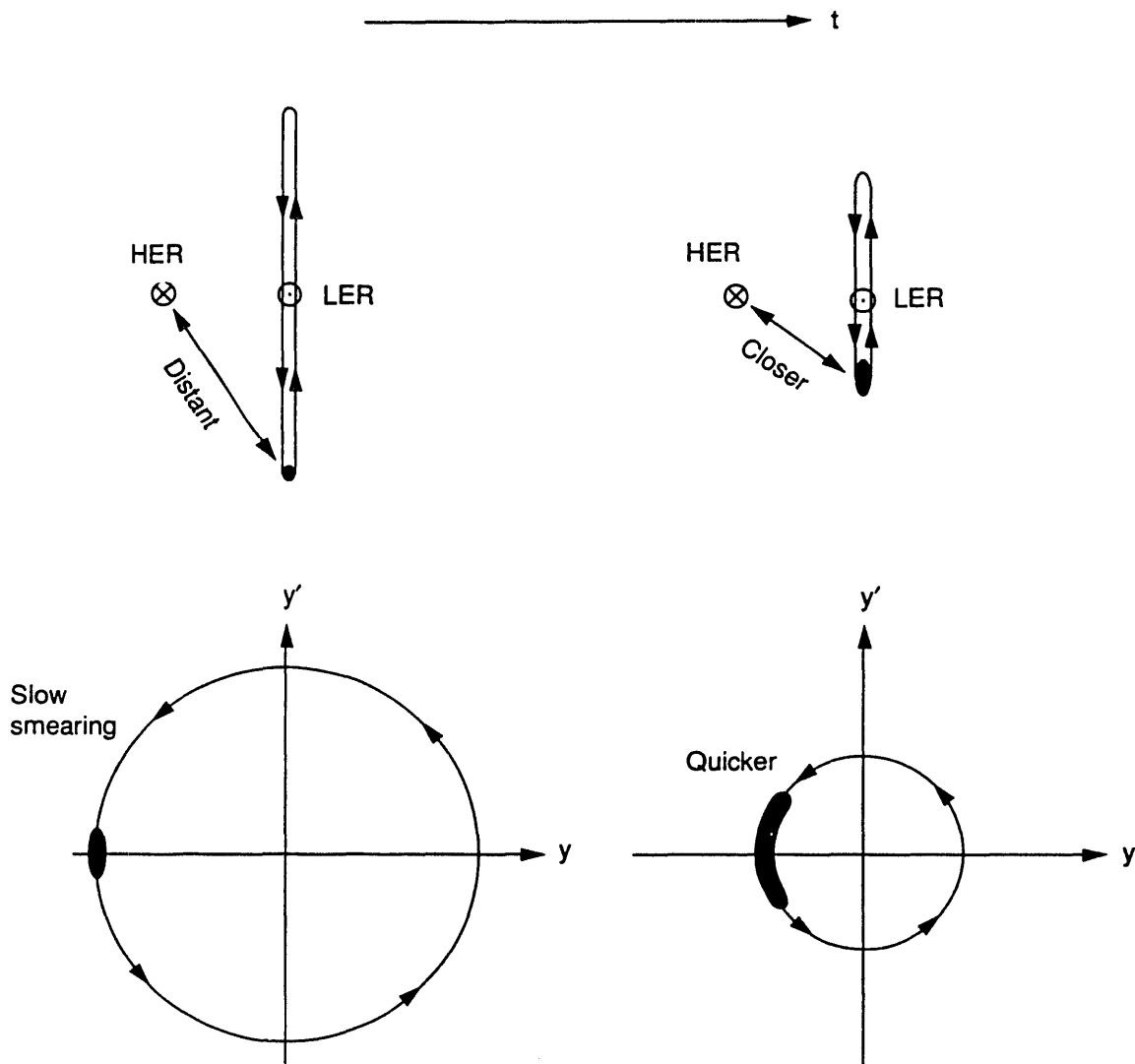


Figure 6. Schematic illustration of the parasitic beam-beam interaction during the vertical injection process.

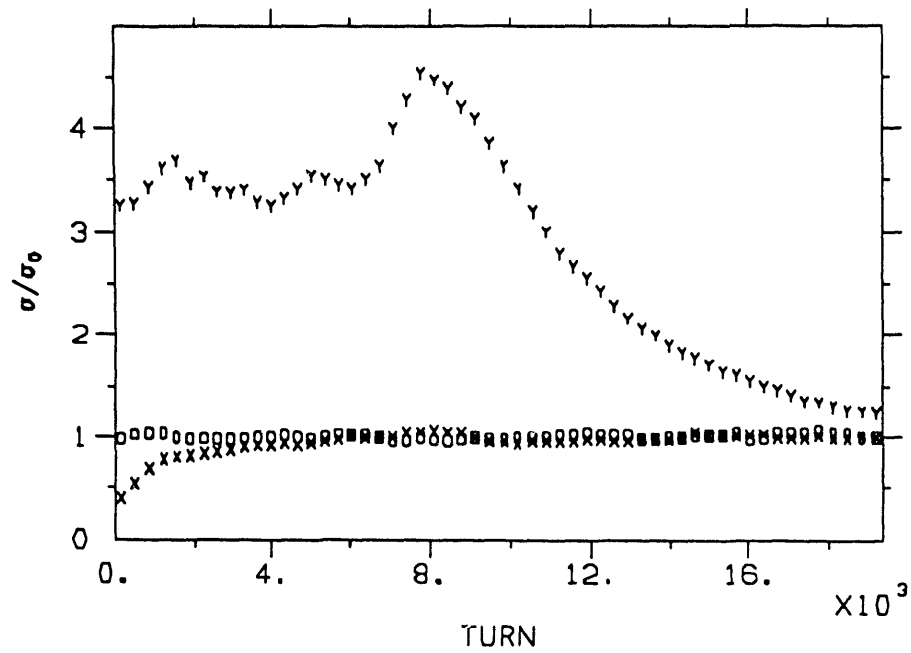


Figure 7. The time evolution of the injected beam sizes in units of the nominal storage ring beam sizes during the vertical injection process (x=horizontal, y=vertical, and o=longitudinal).

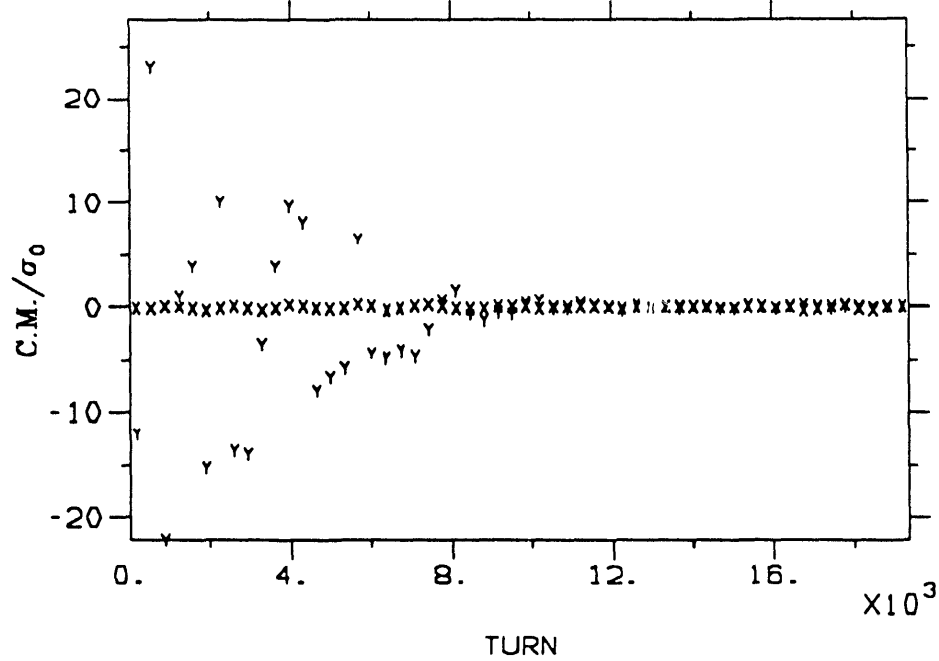


Figure 8. The time evolution of the baricentroid positions of the injected beam in units of the nominal storage ring beam sizes during the vertical injection process (x=horizontal, and y=vertical).

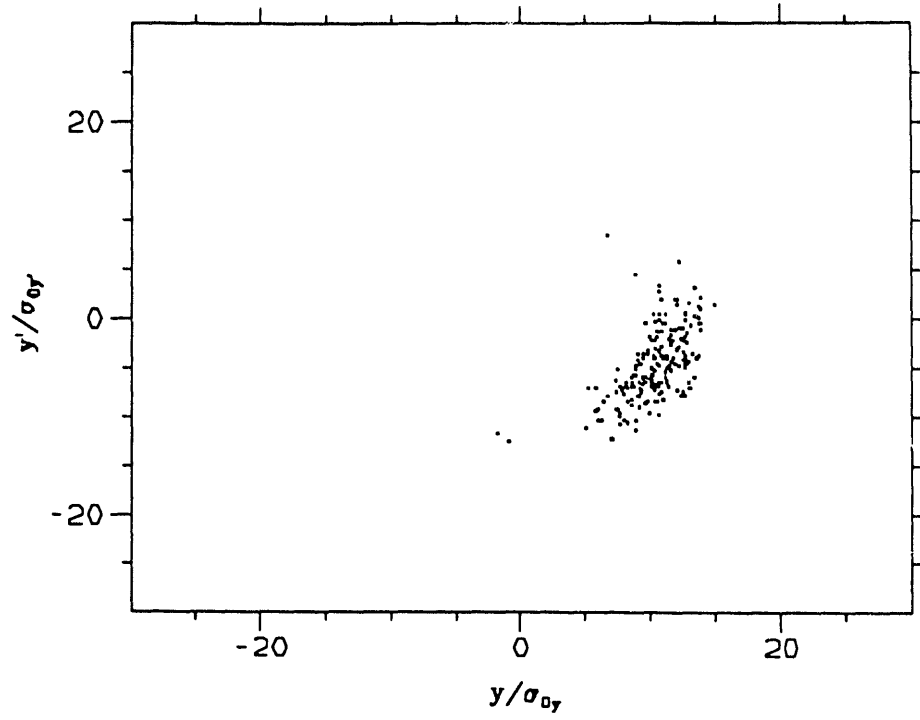


Figure 9(a). The vertical distribution of the injected beam in normalized phase space after 4000 turns.

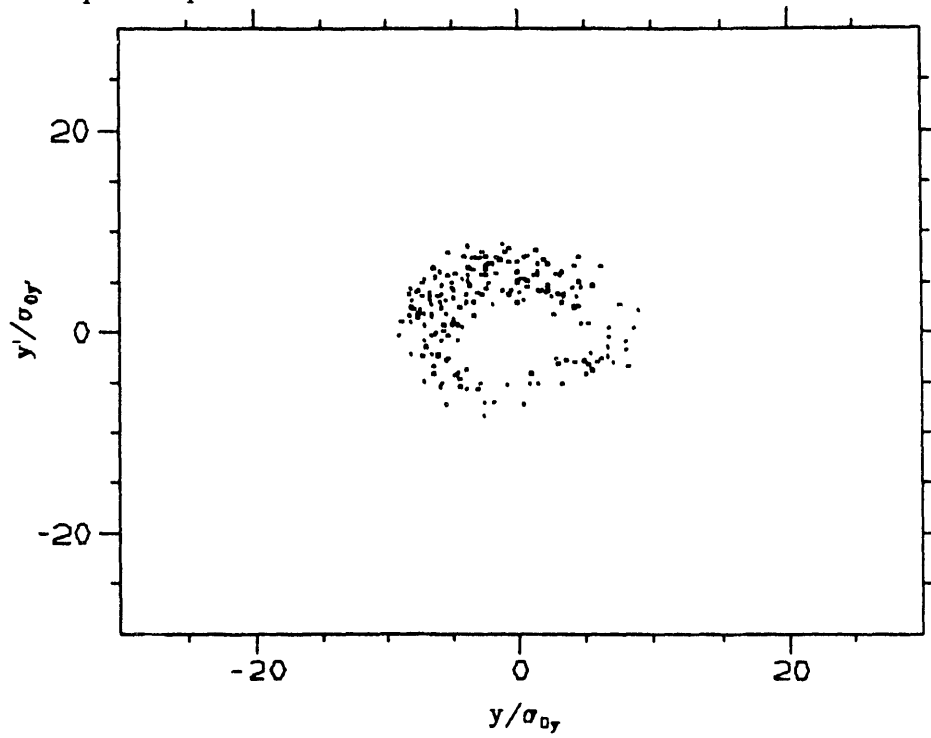


Figure 9(b). The vertical distribution of the injected beam in normalized phase space after 8000 turns.

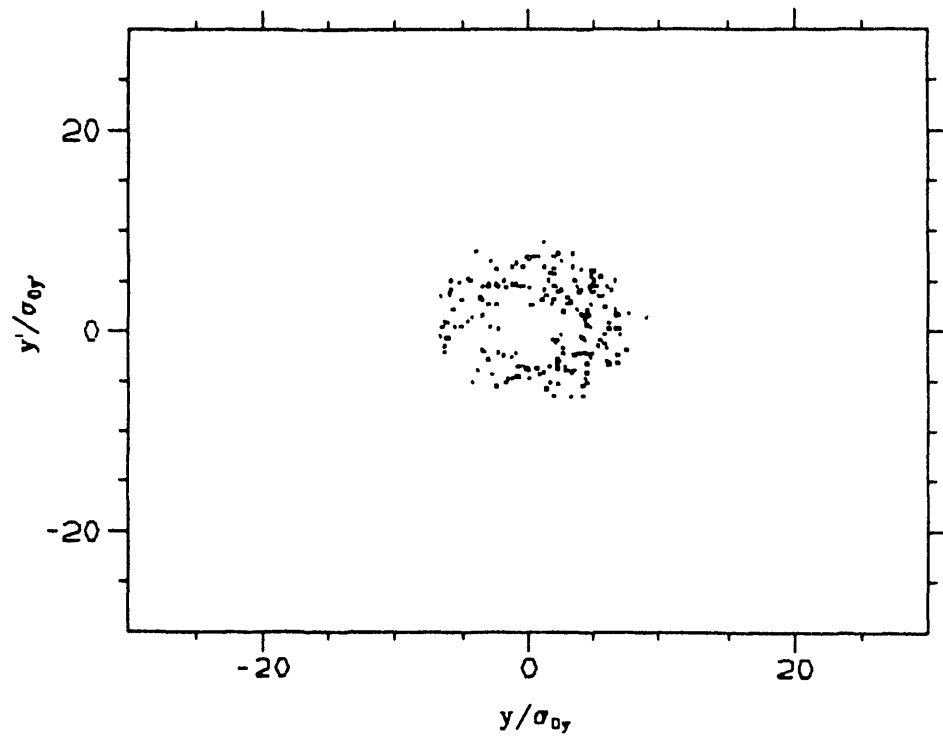


Figure 9(c). The vertical distribution of the injected beam in normalized phase space after 10000 turns.

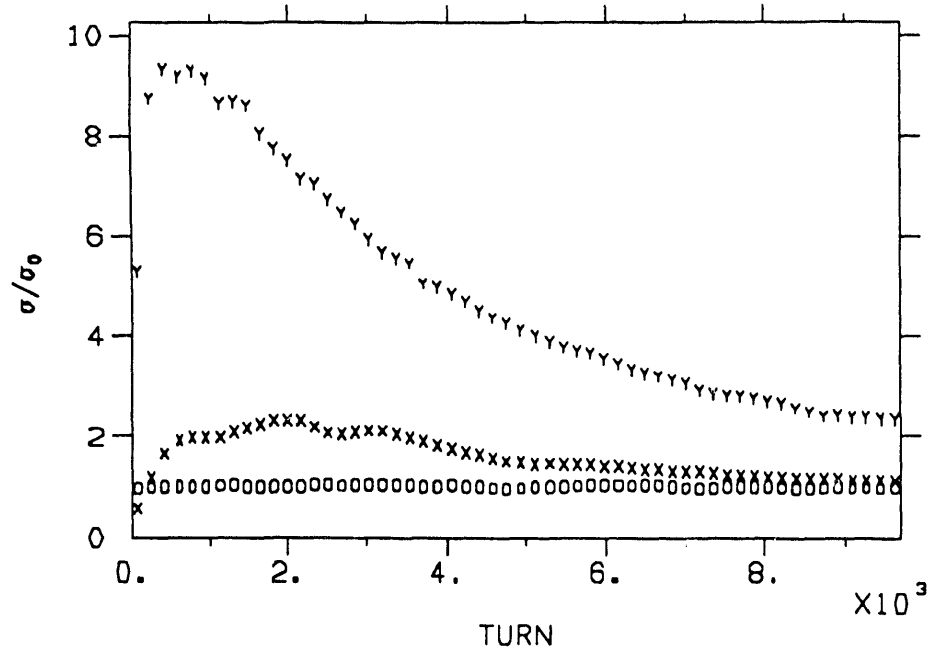


Figure 10(a). The time evolution of the injected beam sizes in units of the nominal storage ring beam sizes for the vertical separation $d_y = 4\sigma_{0x,+}$ at the 1st PC during the horizontal injection process.

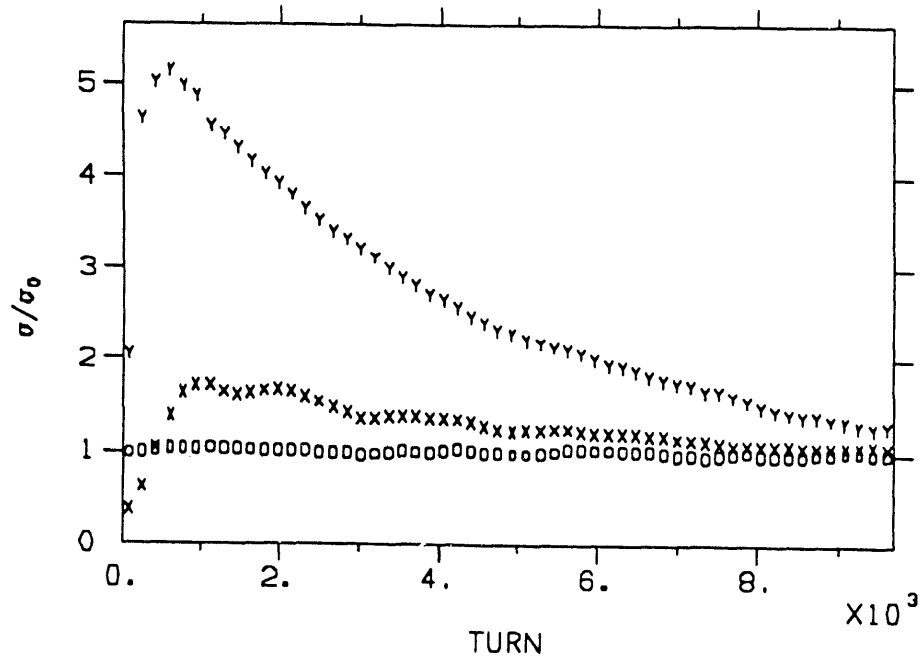


Figure 10(b). The time evolution of the normalized sizes of the injected beam for the vertical separation $d_y = 6\sigma_{0x,+}$.

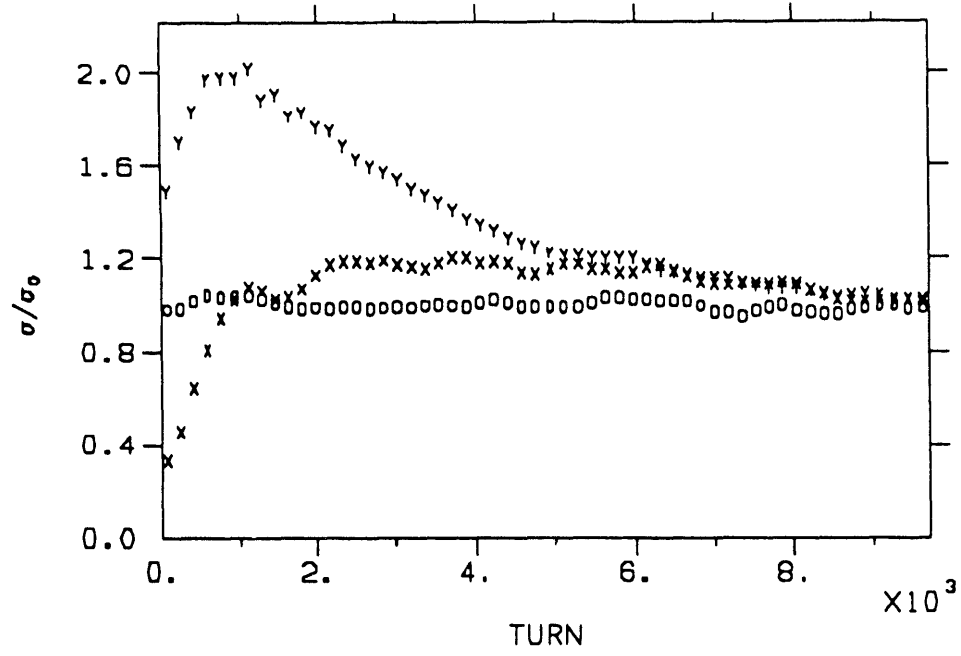


Figure 10(c). The time evolution of the normalized sizes of the injected beam for the vertical separation $d_y = 8\sigma_{0x,+}$.

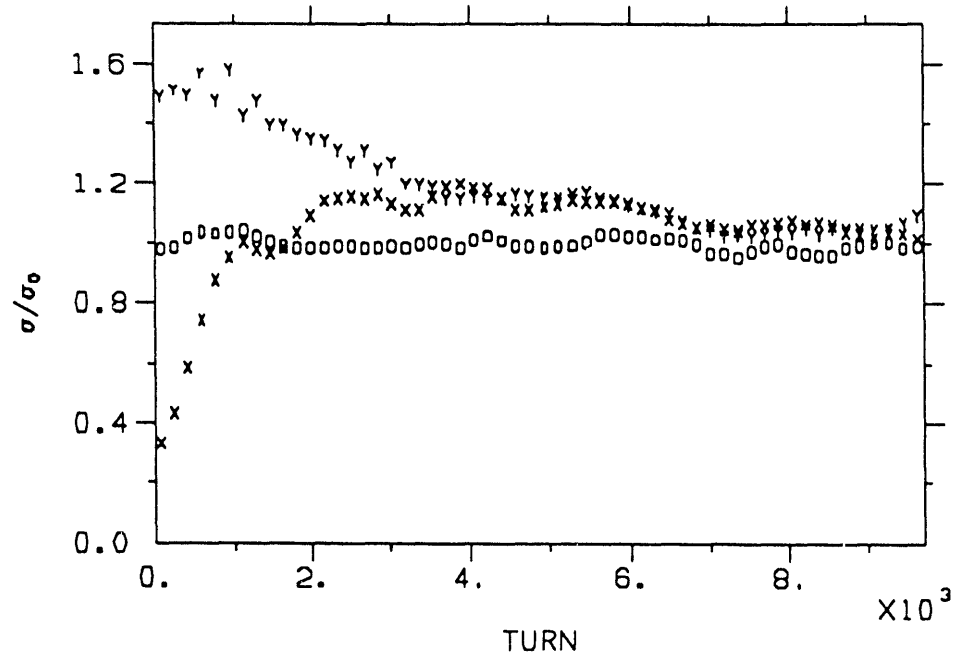


Figure 10(d). The time evolution of the normalized sizes of the injected beam for the vertical separation $d_y = 9\sigma_{0x,+}$.